

Rectifying electrical characteristics of $\text{La}_{0.7}\text{Sr}_{0.3}\text{MnO}_3/\text{ZnO}$ heterostructure

Ashutosh Tiwari,^{a)} C. Jin, D. Kumar, and J. Narayan

Department of Materials Science and Engineering, North Carolina State University, Raleigh, North Carolina 27695-7916

(Received 10 January 2003; accepted 27 June 2003)

We have fabricated a p - n junction, consisting of p -type manganite ($\text{La}_{0.7}\text{Sr}_{0.3}\text{MnO}_3$) and n -type ZnO layers grown on sapphire substrate. This junction exhibits excellent rectifying behavior over the temperature range 20–300 K. Electrical characteristics of $\text{La}_{0.7}\text{Sr}_{0.3}\text{MnO}_3$ (LSMO) film in this heterostructure are found to be strongly modified by the built-in electric field at the junction. It has been shown that by applying the external bias voltage, the thickness of the depletion layer, and hence, the electrical and magnetic characteristics of LSMO film can precisely be modified. © 2003 American Institute of Physics. [DOI: 10.1063/1.1605801]

During the last few years, transition metal oxides have attracted considerable scientific and technological attention.^{1–5} Among those oxides, colossal magnetoresistive manganites of the type $\text{La}_{1-x}\text{A}_x\text{MnO}_3$ (A: Ca, Sr, Ba, etc.) hold special promise. It has been shown earlier that the electrical and magnetic characteristics of manganites are very sensitive function of carrier concentration. The parent compound⁶ ($x=0$) LaMnO_3 is an antiferromagnetic insulator while hole doped manganites⁷ undergo metal–insulator and ferroparamagnetic transitions at temperatures T_c and T_p , respectively, where T_c is close to T_p . By changing the doping concentration, the electrical and magnetic characteristics of manganites can be tuned as per the specific device requirements.

Formation of heterostructure provides another efficient method^{8,9} to control carrier concentration through the modulation of interfacial electronic band. Recently we have fabricated a $\text{La}_{0.7}\text{Sr}_{0.3}\text{MnO}_3$ (LSMO)/ZnO heterostructure to precisely control electrical and magnetic characteristics of LSMO film. Our approach is based on the fact that in LSMO charge carriers are holes while in ZnO electrons are the dominant charge carriers. So if we make a junction of LSMO and ZnO, a thin depletion layer will be formed at the junction. Thickness of this layer and, hence, the carrier concentration in the system can be modulated by applying the external bias across the junction. ZnO was chosen as the counter electrode because:¹⁰ (i) under the normal conditions of deposition it tends to be oxygen deficient and exhibits n -type behavior, and (ii) by changing the oxygen stoichiometry it is possible to have a control over carrier concentration.

Thin film deposition was performed in two steps by using a multitarget pulsed laser deposition chamber with a KrF excimer laser (Lambda Physik 210, $\lambda = 248$ nm). In first step a thin layer (200 nm) of ZnO was deposited on polished sapphire substrate at 650 °C in the oxygen pressure of 1×10^{-5} Torr. In the second step a part of this film was masked and then LSMO film (100 nm) was deposited at 680 °C in the oxygen pressure of 1×10^{-2} Torr. In both of the cases energy density and pulse frequency were 1.5–3 J/cm² and 10 Hz, respectively. In order to investigate the

effect of film thickness of LSMO on its physical properties we deposited two more heterostructures with 5- and 20-nm-thick LSMO films. The crystal structure of all these films was determined by x-ray diffraction using an x-ray diffractometer with Cu K_α radiation and a Ni filter. Electrical measurements were performed by four point probe method using a HP semiconductor parameter analyzer, a Keithly 220 current source, and a Keithly 180 nanovoltmeter. Electrical contacts were made using silver paste and gold wires. Carrier concentration in these films was determined by room temperature Hall measurement. Carrier concentration in ZnO and LSMO films were estimated to be $\sim 1.2 \times 10^{20}/\text{cm}^3$ and $1.8 \times 10^{22}/\text{cm}^3$, respectively.

X-ray diffraction pattern of LSMO/ZnO/sapphire heterostructure is shown in Fig. 1. In the 2θ range 20°–100°, we observed the peaks corresponding to (0002) and (0004) planes of ZnO, (0006) and (00012) planes of sapphire, and (100), (200), (110), and (220) planes of LSMO. This suggests that ZnO grows epitaxially on sapphire with preferred c -axis orientation while LSMO film is polycrystalline. Out-of-plane lattice parameter for LSMO is determined to be 3.87 Å which is in good agreement with the earlier reports.¹¹ In order to get more precise information about the crystalline quality and the nature of ZnO/LSMO interface we performed transmission electron microscopic investigation on this heterostructure. Figure 2(a) shows a typical low magnification cross-sectional transmission electron microscopy (TEM) im-

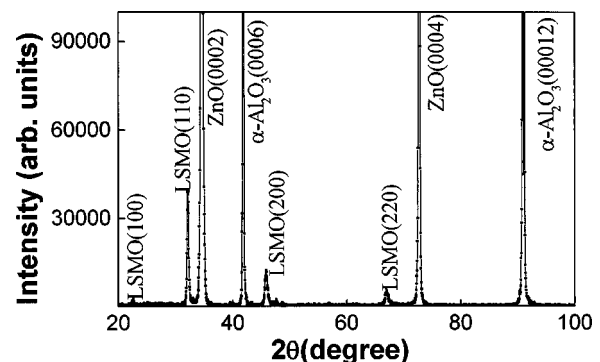


FIG. 1. X-ray diffraction pattern of $\text{La}_{0.7}\text{Sr}_{0.3}\text{MnO}_3/\text{ZnO}$ heterostructure on sapphire substrate.

^{a)}Electronic mail: atiwari@unity.ncsu.edu

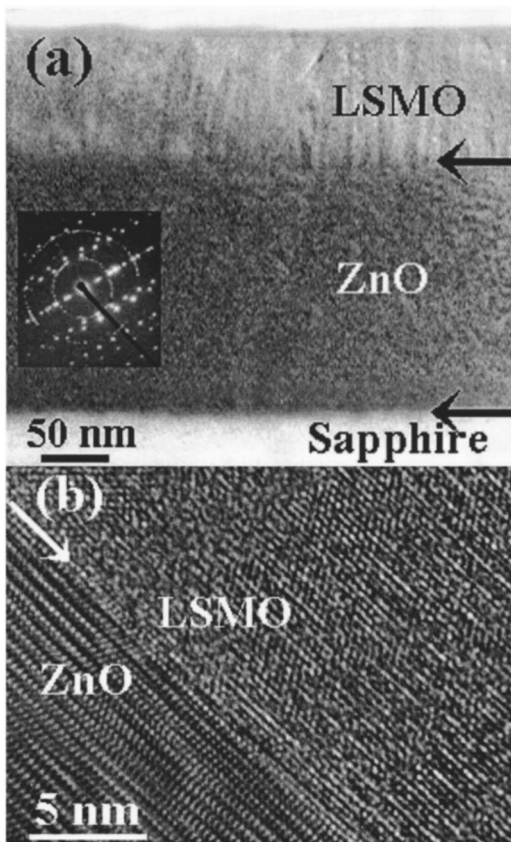


FIG. 2. Typical cross-sectional TEM image of $\text{La}_{0.7}\text{Sr}_{0.3}\text{MnO}_3/\text{ZnO}/\text{sapphire}$ heterostructure along $(2\bar{1}\bar{1}0)$ direction of sapphire (a) low magnification image and the corresponding SAED (inset) and (b) high-resolution TEM image of the ZnO/LSMO interface.

age of ZnO/LSMO/sapphire heterostructure along $(2\bar{1}\bar{1}0)$ direction of sapphire substrate. The inset of this figure shows the corresponding selected area electron diffraction (SAED). This pattern contains diffraction spots corresponding to epitaxial ZnO and sapphire and circular diffraction rings corresponding to polycrystalline LSMO. Figure 2(b) shows the high-resolution image of ZnO/LSMO interface. As can be seen from this figure interface between ZnO and LSMO is atomically sharp with no evidence of any significant interdiffusion.

Figure 3 shows the I - V characteristics of LSMO/ZnO structure measured in current perpendicular to plane geometry (see inset) at different temperatures. For the sake of

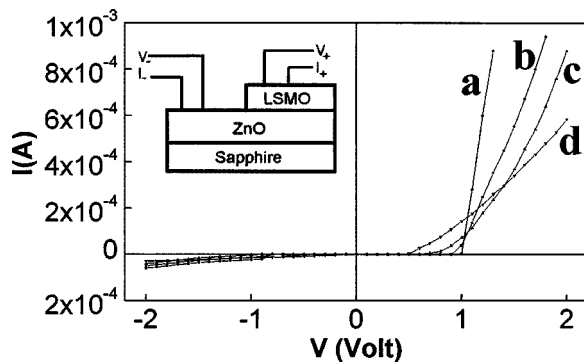


FIG. 3. I - V characteristics of $\text{La}_{0.7}\text{Sr}_{0.3}\text{MnO}_3/\text{ZnO}$ heterojunction at (a) 20, (b) 100, (c) 200, and (d) 300 K. Inset shows a schematic diagram of the heterostructure and measurement geometry.

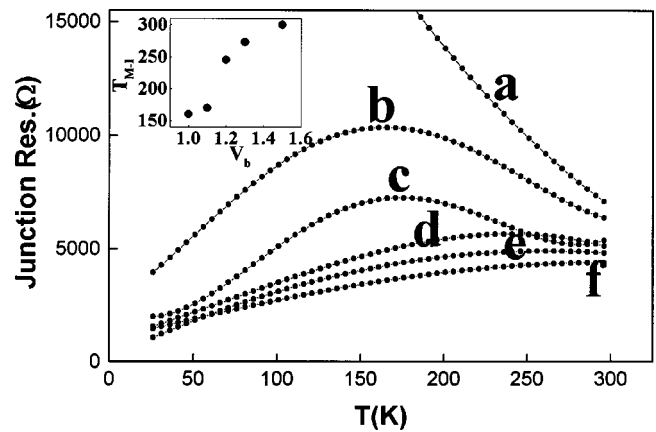


FIG. 4. Junction resistance vs temperature at different bias voltages. (a) 0.8, (b) 1.0, (c) 1.1, (d) 1.2, (e) 1.3, and (f) 1.5 V.

clarity we have shown the I - V curves at $T=20, 100, 200,$ and 300 K only. Asymmetry in I - V curves under forward and reverse bias conditions can clearly be seen. From this curve we found the diffusion potential for LSMO/ZnO heterostructure to be ~ 0.5 eV at 300 K. As it is clear from this figure LSMO/ZnO junction shows rectifying behavior throughout the whole temperature range of our study ($20 \text{ K} < T < 300 \text{ K}$). These characteristics are quite superior to earlier efforts by other groups^{8,12} to make similar kinds of junctions. Two important points which are to be noticed in Fig. 3 are: (i) rectifying behavior occurs over a broad temperature range and (ii) no intermediate insulating layer is required to achieve the rectification.

In Fig. 4 we have shown the variation of junction resistance (R_J) with temperature for different bias voltages. Values of the R_J at different bias voltages were calculated by dividing the value of bias voltage by the current. For $V_{\text{bias}} < 1.0$ V, the junction shows an insulating behavior with a negative temperature coefficient of resistivity throughout the whole temperature range. For higher values of the bias voltage value of the junction resistance goes down and it shows metal-insulator (M - I) transition. Value of the metal-insulator transition temperature T_{M-I} keeps on increasing with increase in bias voltage. In the inset of Fig. 4 we have shown the variation of T_{M-I} with the applied bias voltage. It can clearly be seen that the M - I transition temperature in LSMO film can very precisely be controlled by changing the electric field across the LSMO/ZnO junction. Here it is important to note that in manganites, both metal-insulator transition and ferropararansitions are governed by the double exchange interaction mechanism¹³ and both the phenomenon go hand by hand. This provides us with an excellent opportunity to understand the emergence of ferromagnetism in ultrathin films where the direct measurement of magnetic properties may not be feasible.

Figure 5 shows the temperature dependence of the normalized sheet resistance of LSMO films in LSMO/ZnO heterostructure. As can be seen from this figure, 100-nm-thick LSMO film undergoes M - I transition at $T_{M-I} \sim 260$ K. This value of T_{M-I} is much smaller than the corresponding value observed in bulk LSMO sample.³ For 20-nm-thick film M - I transition occurs at still lower temperature ($T_{M-I} \sim 105$ K) and for 5-nm-thick films no M - I transition could be observed.

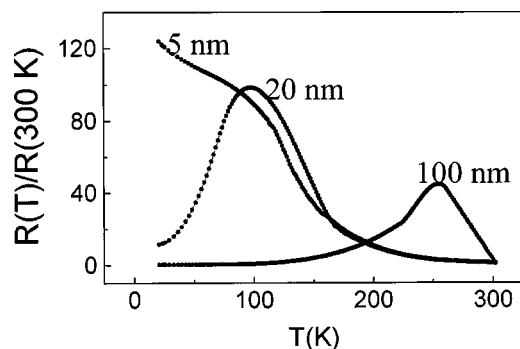


FIG. 5. Normalized sheet resistance of electrical of $\text{La}_{0.7}\text{Sr}_{0.3}\text{MnO}_3$ films in $\text{La}_{0.7}\text{Sr}_{0.3}\text{MnO}_3/\text{ZnO}$ heterojunction.

served down to the lowest temperature (20 K) of our measurement. Reduction in the value of T_{M-I} for LSMO thin films has been observed previously also by several groups.^{14,15} This lowering is normally attributed to the presence of tensile strain in the film. Strain in thin films can arise because of the following two reasons: (a) lattice mismatch between the film and substrate, and/or (b) mismatch of thermal coefficient of expansion (TCE) between the film and substrate. LSMO films in LSMO/ZnO heterostructure are polycrystalline with random in-plane orientation, hence, the lattice mismatch strain is expected to be absent in the film. However, since TCE of LSMO¹⁶ ($11.2 \times 10^{-6} \text{ K}^{-1}$) is much higher than that of ZnO¹⁰ ($2.9 \times 10^{-6} \text{ K}^{-1}$), a significant amount of tensile strain is likely to be present in LSMO films. This tensile strain may be one cause of the observed lowering of T_{M-I} in LSMO films. Another factor that may be responsible for this behavior is the onset of a depletion layer at the ZnO/LSMO interface. Because of this depletion layer the effective carrier concentration in LSMO film may get reduced which may consequently lower T_{M-I} . In the case of thinner films the effect of the depletion layer is expected to

be more dominant; if the film is extremely thin, the depletion region may extend over the entire thickness of the film resulting in an overall insulating behavior. However, at this point we want to mention that the exploration of the exact cause of observed electrical resistivity behavior of LSMO in ZnO/LSMO heterostructure needs further investigation.

In conclusion, we have grown rectifying LSMO/ZnO heterojunctions on sapphire substrate using a pulsed excimer laser. These junctions provide an effective way to control the electrical and magnetic characteristics of giant magnetoresistive LSMO films by using the built-in electric field at the LSMO/ZnO interface. They also provide an opportunity to integrate various magnetic and magnetoresistive properties of manganites with nonlinear optical and optoelectronics applications of ZnO.

¹A. Asamitsu, Y. Moritomo, Y. Tomioka, T. Arima, and Y. Tokura, *Nature* (London) **373**, 407 (1995).

²S. Jin, T. H. Tiefel, M. McCormack, R. A. Fastnacht, R. Ramesh, and L. H. Chen, *Science* **264**, 413 (1993).

³A. Tiwari and K. P. Rajeev, *Phys. Rev. B* **60**, 10591 (1999).

⁴J. Zhang, H. Tanaka, and T. Kawai, *Appl. Phys. Lett.* **80**, 4378 (2002).

⁵A. Tiwari, K. P. Rajeev, and J. Narayan, *Solid State Commun.* **121**, 357 (2002).

⁶R. Von Helmolt, J. Wecker, B. Holzapfel, L. Schultz, and K. Samwer, *Phys. Rev. Lett.* **71**, 2331 (1994).

⁷S. E. Lofland, S. M. Bhagat, H. L. Ju, G. C. Xiong, T. Venkatesan, and R. L. Greene, *Phys. Rev. B* **52**, 15058 (1995).

⁸H. Katsu, H. Tanaka, and T. Kawai, *Appl. Phys. Lett.* **76**, 3245 (2000).

⁹H. Tanaka, J. Zhang, and T. Kawai, *Phys. Rev. Lett.* **88**, 027204 (2002).

¹⁰A. Tiwari, M. Park, C. Jin, H. Wang, D. Kumar, and J. Narayan, *J. Mater. Res.* **17**, 2480 (2002).

¹¹A. Tiwari, A. Chugh, C. Jin, D. Kumar, and J. Narayan, *Solid State Commun.* **121**, 679 (2002).

¹²C. Mitra, P. Raychaudhuri, G. Köbernik, K. Dörr, K.-H. Müller, L. Schultz, and R. Pinto, *Appl. Phys. Lett.* **79**, 2408 (2001).

¹³C. Zener, *Phys. Rev.* **82**, 403 (1951).

¹⁴M. Izumi, Y. Konishi, T. Nishihara, S. Hayashi, M. Shinohara, M. Kawasaki, and Y. Tokura, *Appl. Phys. Lett.* **73**, 2497 (1998).

¹⁵T. Kanki, H. Tanaka, and T. Kawai, *Phys. Rev. B* **64**, 224418 (2001).

¹⁶A. Chakraborty and H. S. Maiti, *Ceram. Int.* **25**, 115 (1999).